Effects of Exchange Interaction in Bilayer $Dy_xCo_{1−x}$/NiFe Films in the Vicinity of Compensation Compositions of Amorphous DyCo Alloys

R. S. Iskhakov[1], *, V. A. Seredkin[1], S. V. Stolyar[1, 2],
G. I. Frolov[1], and V. Yu. Yakovchuk[1]

[1] *Kirenskiĭ Institute of Physics, Siberian Division, Russian Academy of Sciences, Krasnoyarsk, 660036 Russia*
[2] *Krasnoyarsk State University, Krasnoyarsk, 660041 Russia*
* e-mail: rauf@iph.krasn.ru
Received September 6, 2004; in final form, October 11, 2004

The displacement field of the hysteresis loop due to exchange anisotropy in planar DyCo/NiFe systems is studied experimentally as a function of the concentration of the rare-earth element. The bilayer DyCo/NiFe film system is characterized by an orthogonal arrangement of the effective magnetizations of separate layers under the condition that the amorphous DyCo layer is prepared in the region of magnetic compensation. An analysis of the dependence of the displacement field on the Dy concentration has led to an understanding of the physical mechanism of the formation of the exchange anisotropy in these planar systems. © 2004 MAIK "Nauka/Interperiodica".

PACS numbers: 75.47.Np; 78.55.Qr; 78.67.Pt

At present, studies of the effects of the exchange interaction at the boundary between two different magnetic ordered systems are experiencing a kind of renaissance (see, e.g., [1–3]). This fact is, in many respects, due to the development of the technology of obtaining new varieties of composites. Thus, the formation of multilayer films from layers of soft and hard ferromagnets has significantly improved the characteristics of planar permanent magnets [4]. The phenomenon of so-called exchange anisotropy [5] caused by the effects of the exchange interaction at the boundary between a ferromagnet and an antiferromagnet, which manifest themselves in a hysteresis loop shift with respect to the origin of the coordinates, turned out to be useful in spintronics and for the development of numerous sensors [6]. The phenomenological description of these effects is rather simple and is based on the suggestion that the magnetic moments at the boundary of the different phases are collinear: $\mathbf{JM_1M_2} = JM_1M_2\cos(M_1\wedge M_2)$. In this light, the result obtained in [7] seems especially remarkable. In this work, exchange anisotropy was observed in bilayer TbFe/NiFe and DyCo/NiFe film systems characterized by the orthogonal arrangement of the effective magnetizations of separate layers under the condition that the amorphous REE–TM layer was synthesized in the region of magnetic compensation. In these planar systems, the ratio of the displacement field H_E of the hysteresis loop to the coercive field H_c (characterizing this field) attains 1200%, whereas this ratio equals ~200% in the widely used NiFe/NiFeMn system. Such large values of the H_E/H_c ratio suggest that

planar (TbFe, DyCo)/NiFe systems can be used in numerous applications (see, e.g., [8]), naturally, under the condition that the physical mechanism of the formation of the exchange anisotropy in these systems is understood.

In our works [9–11], a model of the microheterophase structure of amorphous DyCo alloys was suggested based on the results of measuring the dynamic (and static) magnetic characteristics of these composite systems. The features of the magnetic microstructure of these alloys in the compensation region following from this model allowed a number of experimental results on ferromagnetic resonance (FMR) and spin-wave resonance (SWR). In order to detect these features, we (i) obtained three-layer NiFe/DyCo/NiFe film structures with magnetic anisotropy and an orthogonal orientation of the effective magnetizations of the layers, (ii) studied the FMR and SWR spectra of such structures, and (iii) found that the spin system of amorphous DyCo alloys in the concentration region of the magnetic compensation can be presented as two subsystems such that the magnetization of the TM sublattice dominates in one of them (magnetic nanophase Φ_1) and the magnetization of the REE sublattice dominates in the other (magnetic nanophase Φ_2).

The goal of this work is to demonstrate that the effects of the hysteresis loop shift in planar DyCo/NiFe systems can be explained using this model within the framework of conventional notions.

Actually, the model proposed reflects the main property of the structure of amorphous alloys, namely, their

natural fluctuation (topological and compositional) heterogeneity. It is known that chemical (phase) nanoscale heterogeneities exist in amorphous alloys. The magnitude of the concentration fluctuations on these scales can reach several atomic percent of the average concentration. Therefore, the magnetic microstructure of amorphous ferrimagnetics in the concentration region $x_i \pm \Delta x(r) \ll x_{comp}$, $x_i \pm \Delta x(r) \gg x_{comp}$ will significantly differ from the magnetic microstructure in the concentration region $x_i - \Delta x < x_{comp} < x_i + \Delta x$. The magnetic compensation point x_{comp} itself will be determined in this case by the condition $\langle M \rangle = p\mathbf{M}_{eff}^{(\Phi 1)} + q\mathbf{M}_{eff}^{(\Phi 2)} = 0$, where p and q are the volume fractions of the Φ_1 and Φ_2 nanophases and $\mathbf{M}_{eff}^{(\Phi 1)}$ and $\mathbf{M}_{eff}^{(\Phi 2)}$ are their effective magnetizations at $x_i - \Delta x$ and $x_i + \Delta x$, respectively.

To accomplish this goal, we carried out investigations on the quasistatic magnetization reversal of planar Dy_xCo_{1-x}/NiFe structures at various concentrations x_i of the RE element. It was found that the features of the concentration dependences of the displacement field H_E of the hysteresis loop not only were well described within the framework of the model proposed above but also allowed the value of some parameters of this model to be estimated.

SAMPLE PREPARATION AND EXPERIMENTAL PROCEDURE

Bilayer exchange-coupled $Ni_{80}Fe_{20}/Dy_xCo_{1-x}$ films were obtained by thermal evaporation in a vacuum of 3×10^{-6} Torr by successively sputtering the NiFe and DyCo layers from independent evaporators with a ring cathode onto cover-glass substrates. The thickness of the permalloy layer in the planar system was varied from 40 to 300 nm, and the thickness of the DyCo layer, from 10 to 80 nm. Single-layer Dy_xCo_{1-x} films 70 nm thick were used as reference samples. The amorphous state of DyCo was monitored by electron microscopy, and the thickness and chemical composition of the layers, by x-ray spectroscopic analysis. The following experimental techniques were used: magneto-optical Kerr effect measurements in fields up to 15 kOe, a torque magnetometer in fields up to 12 kOe, and a loop meter with fields up to 250 Oe (applied in the film plane) at the frequency $f = 50$ Hz. The main magnetic characteristics of the reference Dy_xCo_{1-x} films were studied in the Dy concentration region from 17 to 30 at. % (see Fig. 1). The dependences measured indicate that the compensation composition, in our case, is the $Dy_{22}Co_{78}$ alloy. The measurement results also show that the effective magnetization in these films is orthogonal to the plane. This is indicated by the absence of a magneto-optical signal in fields up to 15 kOe at fields oriented in the film plane, the detection of the hysteresis loop with the use of the polar Kerr effect (caused by the normal magnetization component), and the inversion of the
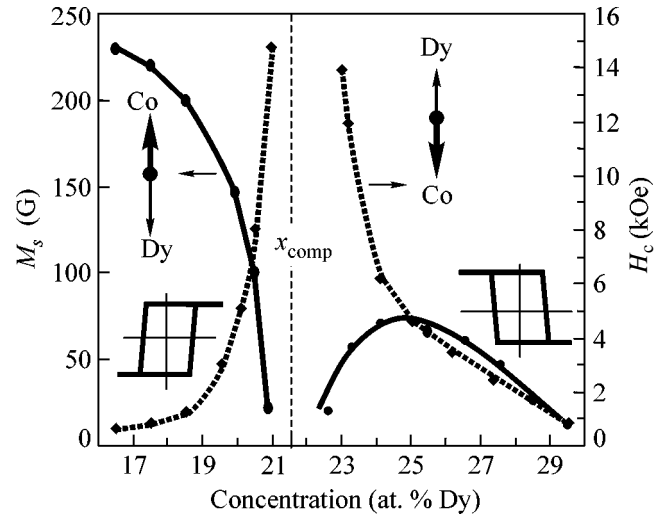
Fig. 1. Concentration dependence of the effective saturation magnetization M_s and the coercive force H_c of amorphous ferrimagnetic Dy_xCo_{1-x} films. The inversion of the form of the magneto-optical signal loop points to the orthogonal orientation of the effective magnetization.

form of the hysteresis loop (see Fig. 1). Measurements on the torque magnetometer allowed the uniaxial anisotropy constant to be evaluated. It was found to be 5×10^{-5}–10^{-6} erg/cm^3 for DyCo films in the concentration region 17–30 at. % Dy, which substantially exceeded the values of $2\pi M_s^2$ presented in Fig. 1. The main magnetic characteristics of the bilayer film structures were also measured as functions of the REE concentration, the thickness of the NiFe layer, and the temperature [12]. Below, as reference values, we will present the results of measuring the hysteresis loop shift field for two series of planar structure samples: substrate/ferrimagnetic Dy_xCo_{1-x} layer (70 nm)/ferromagnetic NiFe layer (150 nm) and substrate/ferromagnetic NiFe layer (150 nm)/ferrimagnetic Dy_xCo_{1-x} layer (70 nm). The ferrimagnetic layer of amorphous DyCo was synthesized with a perpendicular magnetic anisotropy (see Fig. 1), and the ferromagnetic NiFe layer was manufactured with a magnetization in the sample plane oriented along the uniaxial anisotropy (the field $H_k = 7$–8 Oe). This magnetization was formed by applying a constant external magnetic field $H_0 = 50$ Oe in the film plane.

RESULTS AND DISCUSSION

Experimental dependences of the displacement field H_E of the hysteresis loop on the REE concentration in the planar DyCo/NiFe structure and schematic diagrams of the distribution of the Φ_1 and Φ_2 nanophases in the DyCo layer are presented in Fig. 2. The analogous dependence $H_E(x)$ and analogous schematic diagrams for the planar NiFe/DyCo structure are presented
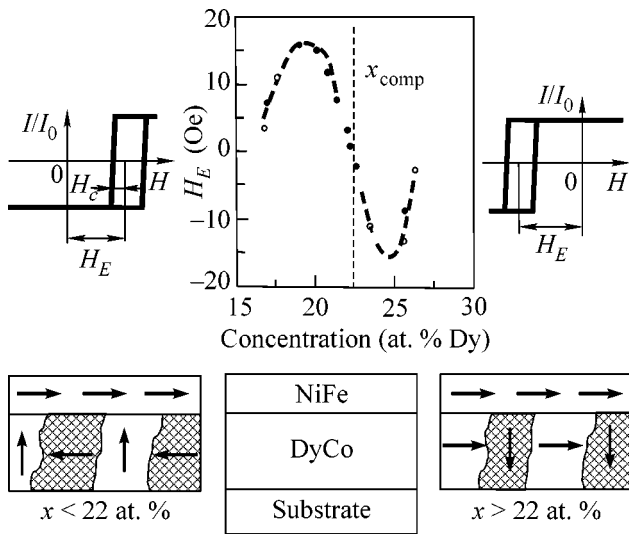
Fig. 2. Hysteresis loops and concentration dependence of the displacement field $H_E(x)$ in exchange-coupled DyCo/NiFe film structures. The schematic diagram presents the orientations of the magnetization vectors of the $3d$ metals of the structures under consideration. In the DyCo layer, the Φ_2 phase ($M_{Co} < M_{Dy}$) is hatched and the Φ_1 phase ($M_{Co} > M_{Dy}$) is not.
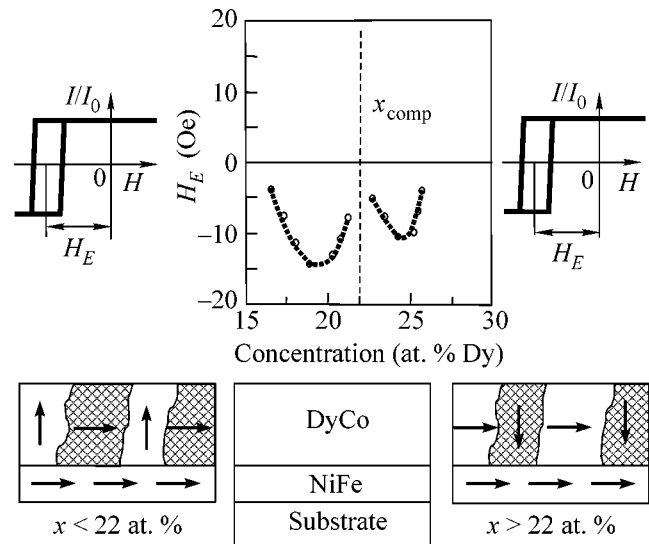
Fig. 3. Hysteresis loops and concentration dependence of the displacement field $H_E(x)$ in exchange-coupled NiFe/DyCo film structures. The schematic diagram presents the orientations of the magnetization vectors of the $3d$ metals of the structures under consideration. In the DyCo layer, the Φ_2 phase ($M_{Co} < M_{Dy}$) is hatched and the Φ_1 phase ($M_{Co} > M_{Dy}$) is not.

in Fig. 3. (The coercive field H_c of the NiFe layer at a selected thickness of 150 nm was 2 Oe and did not depend on either the Dy concentration or the sequence of the layer sputtering.) Let us discuss the similarity and distinction of the presented experimental dependences $H_E(x)$.

In the presented figures, it is evident that the $H_E(x)$ curves are described by different functions, depending on the sequence in which the layers are sputtered: $H_E(x - x_{comp})$ is an antisymmetric function for the Dy_xCo_{1-x}/NiFe films (see Fig. 2), and $H_E(x - x_{comp})$ is a symmetric function for the NiFe/Dy_xCo_{1-x} films (see Fig. 3). However, the singular points of these functions (coordinates of zeros and extremum points) are independent of the sequence of layer sputtering. It is evident that the hysteresis loop shift along the field axis is absent ($H_E = 0$) at $x = x_{comp}$, $x \leq 16$ at. % Dy, $x \geq 27$ at. % Dy in both cases. It is also seen that the displacement fields H_E reach maximum values in these planar structures at $x \approx 19$ at. % for precompensation DyCo compositions and at $x \approx 24$ at. % for postcompensation DyCo compositions.

The results of our experiment are naturally interpreted within the framework of the model of the structure of amorphous DyCo alloys in the region of magnetic compensation proposed in [10] and described at the beginning of this article and also within the framework of the schematic diagrams presented in Figs. 2 and 3. (The arrows here indicate the possible orientation of the magnetization of the $3d$ metals.) Actually, in the range of the REE–TM concentrations $x \leq 16$ at. %

($x \geq 27$ at. %), the magnetic structure of amorphous DyCo is unambiguously attributed to the magnetic Φ_1 (Φ_2) nanophase. Hence, the magnetic moments of the Co sublattice and the Dy sublattice are collinear with the axis perpendicular to the DyCo layer anisotropy, and the effective magnetization vectors of the DyCo and NiFe vectors are mutually orthogonal, which means that magnetic coupling is absent here. A different situation occurs in the concentration region $x_i - \Delta x < x_{comp} < x_i + \Delta x$. Here, the magnetic structure of the DyCo layer is formed by the randomly mixed Φ_1 and Φ_2 nanophases. If the Φ_1 phase belongs to the matrix, the Φ_2 phase is the impurity phase (if Φ_2 is the matrix phase, Φ_1 is the impurity phase). An exception is the compensation point x_{comp}, where the volume fractions of the Φ_1 and Φ_2 nanophases are approximately equal.

For all the concentrations x_i in this region, the effective magnetization of the matrix Φ_i phase in the DyCo layer is aligned with the perpendicular anisotropy field (M_{Co} and M_{Dy} are collinear with this axis, which is detected by the polar Kerr effect). In this case, the magnetization M_{Co} in the impurity Φ_j phase must have an in-plane component because of the strong exchange interaction of the transition elements in the impurity and matrix phases, and the effective magnetization of the Φ_j nanophase gains the possibility of orienting itself along the external field. In our opinion, it is the exchange interaction of M_{Co} in the DyCo layer of the impurity Φ_j phase with the magnetization of the NiFe layer that leads to the exchange anisotropy of NiFe. The

magnitude of this exchange anisotropy, which is characterized by the value of H_E, will be determined by the product of M_{Co} in the impurity Φ_j phase and the area of its contact with the NiFe layer. It is evident from the data presented in Figs. 2 and 3 that this product reaches optimum values at 19 at. % Dy and 24 at. % Dy. At 19 at. % $< x < x_{comp}$ ($x_{comp} < x <$ 24 at. %), the area of the impurity Φ_j phase contact with the NiFe layer continues to grow, but the decrease in H_E indicates that the projection of the magnetization of the Co sublattice onto the plane of the NiFe layer decreases. Finally, at x_{comp}, it follows from the experimental result $H_E = 0$ that the mean value of the projection of the magnetization of the Co sublattices onto the plane of the NiFe layer equals zero, which points to the collinearity of M_{Co} and M_{Dy} with the axis of perpendicular anisotropy.

As the concentration x_i increases (16 at. % $< x_i < x_{comp}$), the morphology of the impurity phase changes: disperse inclusions appear, the number of these disperse inclusions increases, percolation over the disperse inclusions arises, the volume of the formed infinite cluster increases, etc. Therefore, it is natural to associate the singular points of the $H_E(x)$ dependence with the characteristics of this morphological series. In our opinion, the maximum values of H_E correspond to the establishment of percolation over disperse inclusions. Thus, the singular points of the $H_E(x)$ dependences gain an appropriate description within the framework of the proposed model. Also, note that the $H_E(x)$ dependences allow the amplitudes of the concentration fluctuations in DyCo to be evaluated. For example, $|\Delta x| \geq 4$ at. % Dy in the precompensation amorphous DyCo alloy, and $|x| \geq 3$ at. % Dy in the postcompensation amorphous DyCo alloy (see Figs. 2, 3).

Let us show now that the form of these dependences (antisymmetric or symmetric with respect to x_{comp}) is naturally interpreted within the framework of the proposed model. Consider the antisymmetric dependence $H_E(x - x_{comp})$ presented in Fig. 2 and obtained for planar Dy_xCo_{1-x}/NiFe systems. First, the Dy_xCo_{1-x} layer in which the effective magnetization of the main phase is oriented along the perpendicular magnetic anisotropy axis is formed in these planar systems, and the effective magnetization of the impurity phase is oriented in the layer plane. Upon the synthesis of the NiFe layer, a constant field is switched on, and the effective magnetization of the impurity phase in the Dy_xCo_{1-x} layer is oriented along the direction of this field and, hence, along the anisotropy axis formed in NiFe. However, the impurity phase is characterized by the inequality $M_{Co} < M_{Dy}$ in the region $x < x_{comp}$ and by the inequality $M_{Co} > M_{Dy}$ in the region $x > x_{comp}$. The latter means that the magnetization vectors of the Co sublattice and the NiFe layer are anticollinear in the region $x < x_{comp}$, whereas these vectors are unidirectional in the region $x > x_{comp}$ (see the scheme in Fig. 2). It is due to this fact that the displacement field H_E changes its sign at the concentration transition through x_{comp}. The situation is different for the planar NiFe/Dy_xCo_{1-x} system. First, the NiFe layer is formed, in which the external field not only forms uniaxial anisotropy but also determines the direction of the layer magnetization. Next, the field is switched off, and the Dy_xCo_{1-x} layer is synthesized. In this case, only the "exchange field" from the magnetization of the NiFe layer exerts an orienting action on the magnetic moments of the Co sublattice of the impurity phase. Therefore, regardless of the composition of the Dy_xCo_{1-x} layer, the magnetization M_{Co} of the impurity phase and the magnetization of the NiFe layer have the same direction. The latter means that the displacement field H_E will not change its sign when the concentration passes through x_{comp}, which is confirmed by the experimental results (see Fig. 3).

Thus, the physical mechanism of the formation of the exchange anisotropy in bilayer DyCo(TbFe)/NiFe film systems with the orthogonal arrangement of the effective magnetizations of separate layers has been understood in the course of the performed studies. The REE concentrations in the ferrimagnetic layers have been found at which the maximum exchange anisotropy acts on the ferromagnetic layers.

REFERENCES

1. J. Nogues and I. K. Schuller, J. Magn. Magn. Mater. **192**, 203 (1999).
2. A. E. Berkowitz and K. Takano, J. Magn. Magn. Mater. **200**, 552 (1999).
3. P. Grunberg, Acta Mater. **48**, 239 (2000).
4. M. E. McHenry and D. E. Laughlin, Acta Mater. **48**, 223 (2000).
5. W. H. Meiklejohn and C. P. Bean, Phys. Rev. **105**, 904 (1957).
6. R. Jansen, J. Phys. D: Appl. Phys. **36**, R289 (2003).
7. V. A. Seredkin, G. I. Frolov, and V. Yu. Yakovchuk, Pis'ma Zh. Tekh. Fiz. **9** (23), 1446 (1983) [Sov. Tech. Phys. Lett. **9**, 621 (1983)].
8. V. A. Seredkin, S. V. Stolyar, G. I. Frolov, and V. Yu. Yakovchuk, Pis'ma Zh. Tekh. Fiz. **30** (10), 46 (2004) [Tech. Phys. Lett. **30**, 820 (2004)].
9. R. S. Iskhakov, V. Yu. Yakovchuk, S. V. Stolyar, *et al.*, Fiz. Tverd. Tela (St. Petersburg) **43**, 1462 (2001) [Phys. Solid State **43**, 1522 (2001)].
10. R. S. Iskhakov, V. A. Sederkin, S. V. Stolyar, *et al.*, Pis'ma Zh. Éksp. Teor. Fiz. **76**, 779 (2002) [JETP Lett. **76**, 656 (2002)].
11. V. A. Seredkin, R. S. Iskhakov, V. Yu. Yakovchuk, *et al.*, Fiz. Tverd. Tela (St. Petersburg) **45**, 883 (2003) [Phys. Solid State **45**, 927 (2003)].
12. V. Yu. Yakovchuk, Candidate's Dissertation (Krasnoyarsk, 2003).

Translated by A. Bagatur'yants